# Structure, Stability, and Redox Properties of $Mn^{II}$, $Fe^{II}$, $Co^{II}$, and $Co^{III}$ Complexes with 1,3,5-Triamino-1,3,5-trideoxy-*cis*-inositol[1]

**Michele Ghisletta,[2a] Lorenza Hausherr-Primo,[2a] Krisztina Gajda-Schrantz,[2b] Gábor Machula,[2c] László Nagy,[2b] Helmut W. Schmalle,[2d] Greti Rihs,[2e] Frank Endres,[2f] and Kaspar Hegetschweiler*[,2f]**

Laboratorium für Anorganische Chemie, ETH Zentrum, CH-8092 Zürich, Switzerland, Anorganisch-Chemisches Institut der Universität Zürich, Winterthurerstrasse 190, CH-8057 Zürich, Switzerland, Department of Inorganic and Analytical Chemistry, Attila József University, 6701 Szeged, P.O. Box 440, Hungary, Bioinorganic Chemistry Research Group, Hungarian Academy of Sciences, 6701 Szeged, P.O. Box 440, Hungary, Novartis Pharma AG, CH-4002 Basel, Switzerland, and Universität des Saarlandes, Fachrichtung Anorganische Chemie, Postfach 15 11 50, D-66041 Saarbrücken, Germany

*Received September 30, 1997*

The interaction of $Mn^{II}$, $Fe^{II}$, and $Co^{II}$ with the ligand taci (=1,3,5-triamino-1,3,5-trideoxy-*cis*-inositol) was studied in the solid state and in aqueous solution. Magnetic susceptibility measurements revealed a high-spin electron configuration for the Mn and the Fe complexes. Crystal data: $[Mn(taci)_2](NO_3)_2 \cdot 2H_2O$ (**1**), $C_{12}H_{34}MnN_8O_{14}$, monoclinic, space group $P2_1/c$, $a = 7.107(5)$ Å, $b = 8.742(2)$ Å, $c = 18.527(6)$ Å, $\beta = 100.20(4)°$, $Z = 2$; $[Fe(taci)_2]Cl_2 \cdot 6H_2O$ (**2**), $C_{12}Cl_2FeH_{42}N_6O_{12}$, monoclinic, space group $C2/m$, $a = 11.420(2)$ Å, $b = 9.300(2)$ Å, $c = 13.330(3)$ Å, $\beta = 111.97(3)°$, $Z = 2$; $[Co(taci)_2](NO_3)_2 \cdot 1.5H_2O$ (**3**), $C_{12}CoH_{33}N_8O_{13.5}$, monoclinic, space group $P2_1/c$, $a = 7.081(1)$ Å, $b = 8.743(1)$ Å, $c = 18.181(2)$ Å, $\beta = 99.49(1)°$, $Z = 2$. All three structures exhibited distorted octahedral $MN_6$ coordination. The stability constants for the complexes $[M(taci)]^{2+}$ (M = Mn, Fe, Co) and $[M(taci)_2]^{2+}$ (M = Fe, Co) in aqueous media have been evaluated by potentiometric titration. Comparison with other divalent cations showed that the order of stability increases $Mn^{II} < Cd^{II} \approx Fe^{II} < Zn^{II} < Co^{II} < Cu^{II} < Ni^{II}$. In alkaline aqueous media, the complexes **1**−**3** are readily oxidized by dioxygen. The redox properties were analyzed by a series of polarographic and cyclic voltammetric measurements. A new isomeric form of a bis-taci $Co^{III}$ complex was formed, where one of the taci ligands coordinates the metal cation by one nitrogen and two oxygen atoms. The complex was isolated in crystalline form as $[Co(taci)(Htaci)](NO_3)_4 \cdot 0.5H_2O$ (**4**), $C_{12}CoH_{32}N_{10}O_{18.5}$, monoclinic, space group $C2/c$, $a = 30.541(3)$ Å, $b = 9.015(1)$ Å, $c = 17.852(2)$ Å, $\beta = 95.63(1)°$, $Z = 8$. $[Co(tach)(H_2O)_x(NO_3)_{3-x}]^{x+}$ (tach = *all-cis*-1,3,5-triaminocyclohexane, $0 \le x \le 3$) was used as a model to demonstrate that, for $Co^{III}$, the substitution of the three monodentate coligands by a taci molecule resulted generally in an asymmetric binding. An N,O,O and an N,N,O coordination mode were observed for $[Co(taci)(tach)](NO_3)_3 \cdot 3H_2O$ (**5**), and $[Co(H_{-1}taci)(tach)](NO_3)_2 \cdot (3 - x)H_2O \cdot x$MeOH, $0.2 \le x \le 0.5$ (**6**), respectively. Crystal data: **5** ($C_{12}CoH_{36}N_9O_{15}$), monoclinic, $P2_1/n$, $a = 8.942(5)$ Å, $b = 30.07(3)$ Å, $c = 9.354(5)$ Å, $\beta = 109.25(4)°$, $Z = 4$; **6** ($x \approx 0.2$, $C_{12.2}CoH_{35.4}N_8O_{12}$), monoclinic, $P2_1/n$, $a = 7.337(2)$ Å, $b = 19.847(4)$ Å, $c = 15.226(3)$ Å, $\beta = 93.59(3)°$, $Z = 4$.

## Introduction

In previous contributions of this series, we described some of the unique metal binding properties of 1,3,5-triamino-1,3,5-trideoxy-*cis*-inositol (taci),[3−6] which are based on the ability of this ligand to bind a metal center either using oxygen or nitrogen donors (Chart 1). $Ni^{II}$, $Cu^{II}$, $Zn^{II}$, and $Cd^{II}$ are all coordinated exclusively to the nitrogen donors, whereas the alkaline earth metal cations $Mg^{2+}$−$Ba^{2+}$ bind to the neutral oxygen donors.[3,6] For $Al^{III}$, coordination to deprotonated oxygen atoms (zwitterionic form with protonated nitrogen donors) was found.[5] The marked preference of the late divalent transition metal cations for nitrogen donors is well established, and the observed coordination mode is thus not unexpected.[7] It seems, however, that, in the case of $Mn^{II}$ and $Fe^{II}$, binding to a negative oxygen donor is preferred, as exemplified by the substitution of a coordinated amino polycarboxylate by the corresponding polyamine (eq 1, where nta = nitrilotriacetate and tren = tris-(2-aminoethyl)amine). For this system, the following log *K*

$$[M(nta)]^- + tren \rightleftharpoons [M(tren)]^{2+} + nta^{3-} \qquad (1)$$

* To whom correspondence should be addressed.

(1) (a) Dedicated to Professor Paul Saltman on the occasion of his 70th birthday. (b) 1,3,5-Triamino-1,3,5-trideoxy-*cis*-inositol, a Ligand with a Remarkable Versatility for Metal Ions. 8. Part 7: see ref 28.

(2) (a) ETH Zürich. (b) Attila József University (c) Hungarian Academy of Sciences. (d) Universität Zürich. (e) Novartis AG. (f) Universität des Saarlandes.

(3) Hegetschweiler, K.; Gramlich, V.; Ghisletta, M.; Samaras, H. *Inorg. Chem.* **1992**, *31*, 2341.

(4) Ghisletta, M.; Jalett, H.-P.; Gerfin, T.; Gramlich, V.; Hegetschweiler, K. *Helv. Chim. Acta* **1992**, *75*, 2233.

(5) Hegetschweiler, K.; Ghisletta, M.; Fässler, T. F.; Nesper, R.; Schmalle, H. W.; Rihs, G. *Inorg. Chem.* **1993**, *32*, 2032.

(6) Hegetschweiler, K.; Hancock, R. D.; Ghisletta, M.; Kradolfer, T.; Gramlich, V.; Schmalle, H. W. *Inorg. Chem.* **1993**, *32*, 5273.

(7) (a) Mulla, F.; Marsicano, F.; Nakani, B. S.; Hancock, R. D. *Inorg. Chem.* **1985**, *24*, 3076. (b) Hancock, R. D.; Martell, A. E. *Chem. Rev.* **1989**, *89*, 1875.

S0020-1669(97)01242-1 CCC: $15.00 
Published on Web 02/19/1998

**Chart 1**

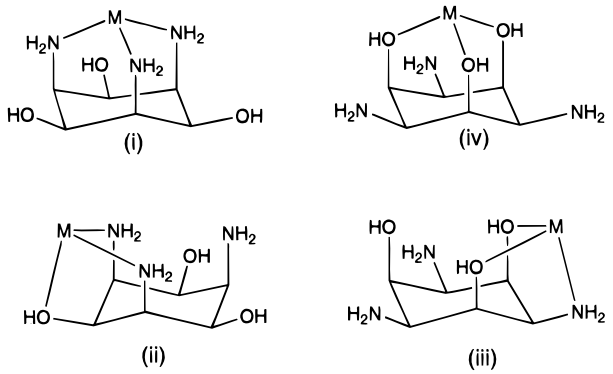


values can be calculated from the corresponding stability constants: $Mn^{II}$, −1.7; $Fe^{II}$, −0.2; $Co^{II}$, +2.3; $Ni^{II}$, +3.1; $Cu^{II}$, +5.7; $Zn^{II}$, +3.8; $Cd^{II}$, +1.9.[8] It is thus less clear whether taci would bind these ions through its oxygen or nitrogen donors.

The chemistry of Mn, Fe, and Co complexes with rigid tridentate ligands which providing exclusively facial N−N−N coordination, has been a subject of considerable attention. Species of this type could serve as promising building blocks for models of Mn and Fe redox enzymes[9] and could also be used as catalysts for low-temperature bleaching.[10] The redox properties of the taci complexes could be of particular interest, since it is possible that a metal center interacts with this ligand in different ways in the different oxidation states, giving rise to the possibility that a redox reaction could be coupled with a change in the coordination sphere.[11] In the current contribution, we report the crystal structures and the stability constants of taci complexes with the divalent $Mn^{II}$, $Fe^{II}$, and $Co^{II}$ and present a preliminary study of the redox properties of these complexes.

## Experimental Section

**Materials and Analyses**. C, H, N analyses were performed by D. Manser (Laboratorium für Organische Chemie, ETH-Zürich). $Mn(ClO_4)_2 \cdot 6H_2O$, $Mn(NO_3)_2 \cdot 4H_2O$, $FeCl_2 \cdot 4H_2O$, $FeSO_4 \cdot 7H_2O$, $CoCl_2 \cdot 6H_2O$, and $Co(NO_3)_2 \cdot 6H_2O$ were from Fluka. A stock solution of $Mn^{2+}_{aq}$, prepared from $Mn(ClO_4)_2 \cdot 6H_2O$ was standardized by complexometric titration. taci was prepared as described previously.[4] taci·$3HNO_3$ was obtained by adding 3 equiv of $HNO_3$ to a solution of taci in MeOH. A white solid precipitated, which was filtered off and dried at 0.1 mbar (ambient temperature). Anal. Calc for $C_6H_{18}N_6O_{12}$: C, 19.68; H, 4.95; N, 22.95. Found: C, 19.55; H, 4.83; N, 22.97. $[Co(taci)_2]Cl_3$ and $[Co(tach)](NO_3)_3$ (dissolved in MeOH, tach = *all-cis*-1,3,5-triaminocyclohexane) were prepared according to published procedures.[4,12] Deoxygenated water was obtained by distillation under Ar. All other chemicals were commercially available compounds of reagent grade quality.

**Electrochemistry and Potentiometry.** Cyclic voltamograms were measured using a three-electrode configuration with a saturated calomel reference electrode (+0.241 V vs SHE), a Pt counter electrode, and a Pt working electrode. The measurements were performed on an EG&G 273 potentiostat in 1.0 M NaCl (aqueous) under Ar at 25 ± 1 °C. The samples were prepared in situ by adding hydrated $MCl_2$ salts (M = Fe, Co) to a taci·3HCl solution. The total M:total taci ratio was 1:3 (total [M] = $5 \times 10^{-3}$ M), and the pH was adjusted to 9.5. Polarograms were recorded on a Radelkis Universal polarograph OH-105. A saturated calomel electrode was used as reference, the mercury height was 55 cm, the capillary constants $m = 2 \times 10$ mg·s$^{-1}$, and $t = 3.2$ s. In all experiments, the [Mn]:[taci] ratio was 1:4 (total [Mn] = $1.22 \times 10^{-3}$ M). Mn was applied either as $Mn^{2+}$ or as a $Mn^{IV}$ complex, which was prepared in situ by passing dioxygen through the sample solution prior to the measurement. The polarograms were evaluated according to the equation $E = E_{1/2} + RT/z\alpha F \ln[(i_d - i)/i]$,[13] where α was derived from a linear regression by plotting $E$ vs $\ln[(i_d - i)/i]$. The range $0.95 < \alpha < 1.05$ was used as criterion for a reversible process.

Potentiometric titrations were performed as described previously at 25.0 ± 0.1 °C and an ionic strength of 0.1 or 1.0 M $KNO_3$.[6] $Mn(NO_3)_2 \cdot 4H_2O$, $FeSO_4 \cdot 7H_2O$, $Co(NO_3)_2 \cdot 6H_2O$, taci·$3HNO_3$, and the corresponding solid taci complexes were used for the preparation of the sample solutions. A $pK_w$ of 13.79(1) was determined by several calibration titrations. All equilibrium constants are reported as concentration quotients, and pH is defined as −log [$H^+$]. The computer programs SUPERQUAD[14] and BEST[15] were used for evaluation.

**Magnetism, Spectroscopy, and Mass Spectrometry.** The magnetic susceptibility of solid $[Mn(taci)_2](NO_3)_2 \cdot 2H_2O$ (**1**) and $[Fe(taci)_2]Cl_2 \cdot 6H_2O$ (**2**) was measured on a MPMS 5 SQUID magnetometer from Quantum Design; no correction was applied for diamagnetism.

UV−vis spectra were recorded on a Uvikon 941 spectrophotometer; maxima are listed in the form $\lambda_{max}$ (nm) ($\epsilon$ ($M^{-1}$ $cm^{-1}$)). $^1H$ and $^{13}C$ NMR spectra were measured on a Bruker AMX 500 spectrometer (500.13 and 125.9 MHz for $^1H$ and $^{13}C$, respectively). Two-dimensional NMR experiments ($^1H-^1H$ COSY) were performed according to the literature.[16] Chemical shifts ($\delta$, in ppm) are given relative to 3-(trimethylsilyl)propionate-$d^4$ (=0 ppm). EPR spectra were recorded on a Bruker ECS 106 spectrometer at 9.165 GHz with 10 mW microwave power and a modulation frequency of 100 kHz. The measurements were carried out on a sample of the $Mn^{II}$−taci complex which was prepared using $2.4 \times 10^{-3}$ M $Mn(ClO_4)_2 \cdot 6H_2O$ and $1.4 \times 10^{-2}$ M of taci and adjusting the pH to 7.9. Sample solutions of higher pH were prepared by adding appropriate amounts of NaOH under an inert atmosphere.

The $FAB^+$ mass spectrometry was performed on a VG ZAB-VSEQ spectrometer, equipped with a VG-$Cs^+$ FAB gun (35 keV, 2 μA beam current). The samples were dissolved in water, and the measurements were made in a glycerol matrix. Data are given as *m*/*z* (%, assignment).

**Preparation of $[Mn(taci)_2](NO_3)_2 \cdot 2H_2O$ (1), $[Fe(taci)_2]Cl_2 \cdot 6H_2O$ (2), and $[Co(taci)_2](NO_3)_2 \cdot 1.5H_2O$ (3).** All operations were performed under argon, and in all cases deoxygenated water was used as solvent. Crystalline samples of **1**−**3** were obtained by the addition of $Mn(NO_3)_2 \cdot 4H_2O$, $FeCl_2 \cdot 4H_2O$, or $Co(NO_3)_2 \cdot 6H_2O$, respectively, to an aqueous solution of taci (1 M) in a 1:2 molar ratio. The solids precipitated immediately from the reaction mixture and were recrystallized from water. Yields fell in the range 60−70%. The crystals proved to be suitable for X-ray analysis.

White crystals of **1** were air stable. Anal. Calc for $C_{12}H_{34}MnN_8O_{14}$: C, 25.31; H, 6.02; N, 19.68. Found for the air-dried product: C, 25.57; H, 6.14; N, 19.48. MS ($FAB^+$, glyc = glycerol): 178.1 (81, $[H(taci)]^+$); 231.0 (26, $[H_{-1}Mn(taci)]^+$); 322.1 (11,

(8) Martell, A. E.; Smith, R. M.; Motekaitis, R. J. Critically Selected Stability Constants of Metal Complexes. *NIST Standard Reference Database 46*, Version 3.0; NIST Standard Reference Data: Gaithersburg, MD 20899, 1997.

(9) (a) Müller, M.; Bill, E.; Weyhermüller, T.; Wieghardt, K. *J. Chem. Soc., Chem. Commun.* **1997**, 705. (b) Bossek, U.; Hummel, H.; Weyhermüller, T. Wieghardt, K.; Russell, S.; van der Wolf, L.; Kolb, U. *Angew. Chem., Int. Ed. Engl*. **1996**, *35*, 1552. (c) Brown, C. A.; Remar, G. J.; Musselman R. L.; Solomon E. I. *Inorg. Chem*. **1995**, *34*, 688. (d) Trofimenko, S. *Chem. Rev*. **1993**, *93*, 943 and references cited therein. (e) Vincent, J. B.; Olivier-Lilley, G. L.; Averill, B. A. *Chem. Rev*. **1990**, *90*, 1447 and references cited therein.

(10) Hage, R.; Iburg, J. E.; Kerschner, J.; Koek, J. H.; Lempers, E. L. M.; Martens, R. J.; Racherla, U. S.; Russell, S. W.; Swarthoff, T.; van Vliet, M. R. P.; Warnaar, J. B.; van der Wolf, L.; Krijnen, B. *Nature* **1994**, *369*, 637 and references cited therein.

(11) Yano, S.; Doi, M.; Tamakoshi, S.; Mori, W.; Mikuriya, M.; Ichimura, A.; Kinoshita, I.; Yamamoto, Y.; Tanase, T. *J. Chem. Soc., Chem. Commun.* **1997**, 997.

(12) Hausherr-Primo, L.; Hegetschweiler, K.; Rüegger, H.; Odier, L.; Hancock, R. D.; Schmalle, H. W.; Gramlich, V. *J. Chem. Soc., Dalton Trans*. **1994**, 1689.

(13) Bard, A. J.; Faulkner, L. R. *Electrochemical Methods Fundamentals and Applications*; John Wiley: New York, 1980; pp 160−170.

(14) Gans, P.; Sabatini, A.; Vacca, A. *J. Chem. Soc., Dalton Trans.* **1985**, 1195.

(15) Motekaitis, R. J.; Martell, A. E. *Can. J. Chem*. **1982**, *60*, 2403.

(16) Jeener, J.; Meier, B. H.; Bachmann P.; Ernst, R. R. *J. Chem. Phys*. **1979**, *71*, 4546.

$[H_{-2}Mn(taci)(glyc)]^+$); 323.1 (44, $[H_{-1}Mn(taci)(glyc)]^+$); 407.1 (35, $[H_{-2}Mn(taci)_2]^+$); 408.1 (100, $[H_{-1}Mn(taci)_2]^+$); 471.1 (11, $[Mn(taci)_2(NO_3)]^+$).

Pale bluish-green crystals of **2** disintegrated rapidly in air (loss of water of crystallization). Moreover, exposure to air resulted in oxidative decomposition. Drying at 100 °C under an atmosphere of He led to a complete dehydration. Anal. Calc for $C_{12}H_{30}Cl_2FeN_6O_6$: C, 29.96; H, 6.28; N, 17.47. Found: C, 29.99; H, 6.30; N, 17.58. MS ($FAB^+$, glyc = glycerol): 178.1 (32, $[H(taci)]^+$); 232.0 (32, $[H_{-1}Fe(taci)]^+$); 324.1 (24, $[H_{-1}Fe(taci)(glyc)]^+$); 408.1 (39, $[H_{-2}Fe(taci)_2]^+$); 409.1 (100, $[H_{-1}Fe(taci)_2]^+$); 445.0 (15, $[Fe(taci)_2Cl]^+$).

Orange crystals of **3** were air stable. Anal. Calc for $C_{12}H_{33}CoN_8O_{13.5}$: C, 25.54; H, 5.89; N, 19.85. Found: C, 25.77; H, 5.78; N, 19.60. MS ($FAB^+$, glyc = glycerol): 178.1 (7, $[H(taci)]^+$); 233.9 (10, $[H_{-2}Co(taci)]^+$); 234.9 (25, $[H_{-1}Co(taci)]^+$); 235.9 (13, $[Co(taci)]^+$); 327.0 (14, $[H_{-1}Co(taci)(glyc)]^+$); 410.1 (12, $[H_{-3}Co(taci)_2]^+$); 411.1 (36, $[H_{-2}Co(taci)_2]^+$); 412.1 (100, $[H_{-1}Co(taci)_2]^+$).

**$[Co(taci)(Htaci)](NO_3)_4\cdot 0.5H_2O$ (4).** $Co(NO_3)_2\cdot 6H_2O$ (0.92 g, 3.15 mmol) dissolved in 25 mL of $H_2O$ was added to a solution of taci (1.12 g, 6.30 mmol) in 25 mL of $H_2O$. An orange solid precipitated, and concentrated $HNO_3$ was added dropwise until a pH of 5 was reached. The solid dissolved, and dioxygen was then passed through the solution for 3 h. A color change from orange to red was noted. The pH was then adjusted to 11 by adding aqueous NaOH, and a second portion of $Co(NO_3)_2\cdot 6H_2O$ (0.92 g, 3.15 mmol) was added. Dioxygen was passed through the solution again for additional 0.5 h. The solution was evaporated under reduced pressure to a total volume of 5 mL and filtered. A 2 mL volume of concentrated $HNO_3$ was added, and a brownish-red solid was precipitated by the addition of EtOH. Recrystallization from $H_2O$/EtOH yielded 0.85 g (1.27 mmol) of **4**. Single crystals were grown by layering a saturated aqueous solution of **4** with EtOH. Anal. Calc for $C_{12}H_{32}CoN_{10}O_{18.5}$: C, 21.47; H, 4.80; N, 20.86. Found: C, 22.00; H, 4.66; N, 20.86. Vis ($H_2O$): 494 (86). $^1$H NMR ($D_2O$):[17] 4.36 (m, 2H), 4.24 (m, 1H), 4.12 (t, $J$ = 3.8 Hz, 2H); 4.02 (t, $J$ = 3.8 Hz, 1 H); 3.62 (t, $J$ = 3.0 Hz, 1H); 3.58 (m, 2H); 3.03 (t, $J$ = 3.8 Hz, 1H); 2.65 (t, $J$ = 3.8 Hz, 2H). $^{13}$C NMR ($D_2O$): 74.9, 70.2, 66.3, 65.9, 64.7, 52.4, 52.2, 51.8. MS ($FAB^+$, glyc = glycerol): 178.1 (100, $[H(taci)]^+$); 235.0 (15, $[H_{-1}Co(taci)]^+$); 236.0 (10, $[Co(taci)]^+$); 326.1 (16, $[H_{-2}Co(taci)(glyc)]^+$); 327.1 (61, $[H_{-1}Co(taci)(glyc)]^+$); 411.1 (25, $[H_{-2}Co(taci)_2]^+$); 412.1 (22, $[H_{-1}Co(taci)_2]^+$).

**$[Co(tach)(taci)](NO_3)_3\cdot 3H_2O$ (5) and $[Co(tach)(H_{-1}taci)](NO_3)_2\cdot(3-x)H_2O\cdot x$MeOH, $0.2 \le x \le 0.5$ (6).** A methanolic solution of $[Co(tach)](NO_3)_3$ (25 mL, 2.5 mmol Co) was added to a slurry of taci (443 mg, 2.5 mmol) in 25 mL of MeOH. The reaction mixture was refluxed for 3 h, stirred at room temperature for an additional 12 h, and allowed to stand for 4 days at 4 °C. The resulting suspension was then separated by filtration. The filtrate was used for the isolation of **6** (see below). The red solid was dried in vacuo, yielding 575 mg (38%) of pure **5**. Single crystals were grown by redissolution in a 1:3 mixture of $H_2O$/EtOH followed by layering with THF. Anal. Calc for $C_{12}H_{36}CoN_9O_{15}$: C, 23.81; H, 5.99; N, 20.82. Found: C, 23.97; H, 5.73; N, 20.53. Vis ($H_2O$): 498 (76). $^1$H NMR ($D_2O$, pD 6.1):[17] 4.16 (m, 1H); 4.07 (m, 2 H); 3.44 (t, $J$ = 2.9 Hz, 1H); 3.37 (t, $J$ = 2.8 Hz, 2H); 3.01 (m, 1H); 2.86 (m, 2H); 1.69−2.07 (m, 6H). $^{13}$C NMR ($D_2O$, pD 6.1): 74.9, 71.0, 67.4, 53.2, 43.3, 43.1, 34.3, 33.9.

The filtrate from the above-mentioned reaction mixture was evaporated under reduced pressure to a total volume of about 5 mL and was allowed to stand for 3 days at 4 °C. The resulting orange solid was filtered off. Yield: 192 mg (14%) of **6**. Single crystals were grown by redissolving the solid in a 1:3 mixture of $H_2O$/EtOH and layering the solution with THF. A variable amount (=$x$, $0.2 \le x \le 0.5$) of MeOH was found to be incorporated in the crystals. It was determined individually for each sample by NMR spectrometry. Anal. Calc. for $C_{12.2}H_{35.4}CoN_8O_{12}$ ($x \approx 0.2$): C, 26.88; H, 6.54; N, 20.55. Found: C, 26.61; H, 6.32; N, 20.05. Vis ($H_2O$): 484 (64), 379 (136). $^1$H NMR ($D_2O$):[17] 3.89 (t, $J$ = 4.0 Hz, 2H); 3.71 (t, $J$ = 4.0 Hz, 1H); 3.36 (t, $J$ = 4.0 Hz, 1H); 3.04 (m, 4H); 2.94 (t, $J$ = 2.9 Hz, 1H); 1.69−2.15 (m, 6H); an additional singlett of MeOH was observed at 3.34 ppm. $^{13}$C NMR ($D_2O$, pD 6.1): 87.0, 72.9, 66.9, 63.4, 49.0, 48.6, 40.3, 40.0.

(17) For the coordinated $NH_2$ groups of **4**−**6**, slow H/D exchange is observed under acidic conditions and additional signals may be observed in the $^1$H-NMR spectrum of a freshly prepared sample (e.g. at 4.47 and 3.59 ppm for **5**). However, heating of the sample (4 h, 60 °C) resulted in the complete disappearance of these signals. The H/D exchange for the OH and the non coordinating $NH_2$/$NH_3$ groups is generally fast in $D_2O$. The NMR spectroscopic properties reported in this paper refer to species where a complete exchange of H versus D was ensured for all these non H(−C) protons.

**Table 1.** Crystallographic Data for $[Mn(taci)_2](NO_3)_2\cdot 2H_2O$ (**1**), $[Fe(taci)_2]Cl_2\cdot 6H_2O$ (**2**), and $[Co(taci)_2](NO_3)_2\cdot 1.5H_2O$ (**3**)

| | complex | | |
|---|---|---|---|
| | **1** | **2** | **3** |
| chem formula | $C_{12}H_{34}MnN_8O_{14}$ | $C_{12}Cl_2FeH_{42}N_6O_{12}$ | $C_{12}CoH_{33}N_8O_{13.5}$ |
| fw | 569.39 | 589.25 | 564.38 |
| space group | $P2_1/c$ (No. 14) | $C2/m$ (No. 12) | $P2_1/c$ (No. 14) |
| $a$, Å | 7.107(5) | 11.420(2) | 7.081(1) |
| $b$, Å | 8.742(2) | 9.300(2) | 8.743(1) |
| $c$, Å | 18.527(6) | 13.330(3) | 18.181(2) |
| $\beta$, deg | 100.20(4) | 111.97(3) | 99.49(1) |
| $V$, Å$^3$ | 1132.9(9) | 1312.9(5) | 1110.2(2) |
| $Z$ | 2 | 2 | 2 |
| $T$, K | 295(2) | 293(2) | 293(2) |
| $\lambda$, Å | 0.710 73 | 0.710 73 | 0.710 73 |
| $\rho_{calc}$, g cm$^{-3}$ | 1.67 | 1.49 | 1.69 |
| $\mu$, cm$^{-1}$ | 6.69 | 8.41 | 8.53 |
| $R$ $[I > 2\sigma(I)]^a$ | 0.036 | 0.078 | 0.049 |
| $R_w$ $[I > 2\sigma(I)]^b$ | | 0.085 | |
| w$R_2$ (all data)$^c$ | 0.113 | | 0.146 |

$^a$ $R = \sum||F_o| - |F_c||/\sum|F_o|$. $^b$ $R_w = [\sum w(|F_o| - |F_c|)^2/\sum wF_o^2]^{1/2}$. $^c$ w$R_2$ $= [\sum w(F_o^2 - F_c^2)^2/\sum wF_o^4]^{1/2}$.

**Table 2.** Crystallographic Data for $[Co(taci)(Htaci)](NO_3)_4\cdot 0.5H_2O$ (**4**), $[Co(taci)(tach)](NO_3)_3\cdot 3H_2O$ (**5**), and $[Co(H_{-1}taci)(tach)](NO_3)_2\cdot 2.8H_2O\cdot 0.2$MeOH (**6**)

| | complex | | |
|---|---|---|---|
| | **4** | **5** | **6** |
| chem formula | $C_{12}CoH_{32}N_{10}O_{18.5}$ | $C_{12}CoH_{36}N_9O_{15}$ | $C_{12.2}CoH_{35.4}N_8O_{12}$ |
| fw | 671.4 | 605.4 | 545.2 |
| space group | $C2/c$ (No. 15) | $P2_1/n$ (No. 14) | $P2_1/n$ (No. 14) |
| $a$, Å | 30.541(3) | 8.942(5) | 7.337(2) |
| $b$, Å | 9.015(1) | 30.07(3) | 19.847(4) |
| $c$, Å | 17.852(2) | 9.354(5) | 15.226(3) |
| $\beta$, deg | 95.63(1) | 109.25(4) | 93.59(3) |
| $V$, Å$^3$ | 4891.4(9) | 2374(3) | 2212.8(9) |
| $Z$ | 8 | 4 | 4 |
| $T$, K | 293(2) | 293(2) | 293(2) |
| $\lambda$, Å | 0.710 73 | 0.710 73 | 0.710 73 |
| $\rho_{calc}$, g cm$^{-3}$ | 1.82 | 1.69 | 1.64 |
| $\mu$, cm$^{-1}$ | 8.12 | 8.15 | 8.55 |
| $R$ $[I > 2\sigma(I)]^a$ | 0.0431 | 0.046 | 0.049 |
| $R_w$ $[I > 2\sigma(I)]^b$ | | 0.048 | |
| w$R_2$ (all data)$^c$ | 0.138 | | 0.145 |

$^a$ $R = \sum||F_o| - |F_c||/\sum|F_o|$. $^b$ $R_w = [\sum w(|F_o| - |F_c|)^2/\sum wF_o^2]^{1/2}$. $^c$ w$R_2$ $= [\sum w(F_o^2 - F_c^2)^2/\sum wF_o^4]^{1/2}$.

**Single-Crystal X-ray Diffraction Studies.** Crystal data for **1**−**6** are presented in Tables 1 and 2, respectively. Atomic coordinates are available as Supporting Information. Selected bond distances and bond angles are listed in Tables 3 and 4. X-ray data were collected at ambient temperature using graphite-monochromatized Mo Kα radiation. The stability of the crystals was checked by measuring standard reflections during data collection; however, no significant loss of intensity was noted for any of the crystals. Corrections for Lorentz and polarization effects were always applied to the data. Additional information on data collection, structure solution, and refinement is summarized below.

Data for **1** were collected on an Enraf-Nonius CAD-4 four-circle diffractometer. A face indexed, numerical absorption correction was applied. The structure was solved by the Patterson routine of SHELXTL PLUS.[18] The non-hydrogen atomic positions were refined with anisotropic displacement parameters (on $F^2$) using SHELXL-93.[19]

**Table 3.** Selected Bond Lengths (Å) and Angles (deg) of $[Mn(taci)_2](NO_3)_2 \cdot 2H_2O$ (**1**), $[Fe(taci)_2]Cl_2 \cdot 6H_2O$ (**2**), and $[Co(taci)_2](NO_3)_2 \cdot 1.5H_2O$ (**3**) with Esd's in Parentheses[a]

| | | | |
|---|---|---|---|
| | $[Mn(taci)_2](NO_3)_2 \cdot 2H_2O$ (**1**) | | |
| Mn−N(1) | 2.271(1) | Mn−N(3) | 2.270(2) |
| Mn−N(5) | 2.249(1) | N(1)−C(1) | 1.473(2) |
| N(3)−C(3) | 1.477(2) | N(5)−C(5) | 1.479(2) |
| O(2)−C(2) | 1.426(2) | O(4)−C(4) | 1.433(2) |
| O(6)−C(6) | 1.421(2) | | |
| N(1)−Mn−N(1a) | 180.0 | N(1)−Mn−N(3) | 85.12(5) |
| N(1)−Mn−N(3a) | 94.88(5) | N(1)−Mn−N(5) | 84.28(5) |
| N(1)−Mn−N(5a) | 95.72(5) | N(3)−Mn−N(3a) | 180.0 |
| N(3)−Mn−N(5) | 85.49(6) | N(3)−Mn−N(5a) | 94.51(6) |
| N(5)−Mn−N(5a) | 180.0 | C(1)−N(1)−Mn | 118.08(9) |
| C(3)−N(3)−Mn | 117.64(9) | C(5)−N(5)−Mn | 118.37(9) |
| | $[Fe(taci)_2]Cl_2 \cdot 6H_2O$ (**2**) | | |
| Fe−N(1) | 2.253(10) | Fe−N(3) | 2.185(6) |
| N(1)−C(1) | 1.47(2) | N(3)−C(3) | 1.47(1) |
| O(2)−C(2) | 1.43 (1) | O(4)−C(4) | 1.45(1) |
| N(1)−Fe−N(3) | 86.1(2) | N(1)−Fe−N(1a) | 180.0 |
| N(1)−Fe−N(3a) | 93.9(2) | N(3)−Fe−N(3a) | 180.0 |
| N(3)−Fe−N(3b) | 91.5(3) | N(3)−Fe−N(3c) | 88.5(3) |
| Fe−N(1)−C(1) | 116.4(6) | Fe−N(3)−C(3) | 117.8(5) |
| | $[Co(taci)_2](NO_3)_2 \cdot 1.5H_2O$ (**3**) | | |
| Co−N(1) | 2.172(2) | Co−N(3) | 2.161(2) |
| Co−N(5) | 2.167(2) | N(1)−C(1) | 1.478(3) |
| N(3)−C(3) | 1.474(3) | N(5)−C(5) | 1.480(3) |
| O(2)−C(2) | 1.403(3) | O(4)−C(4) | 1.436(3) |
| O(6)−C(6) | 1.415(3) | | |
| N(1)−Co−N(1a) | 180.0 | N(1)−Co−N(3) | 86.15(6) |
| N(1)−Co−N(3a) | 93.85(6) | N(1)−Co−N(5) | 86.83(6) |
| N(1)−Co−N(5a) | 93.17(6) | N(3)−Co−N(3a) | 180.0 |
| N(3)−Co−N(5) | 87.66(6) | N(3)−Co−N(5a) | 92.34(6) |
| N(5)−Co−N(5a) | 180.0 | C(1)−N(1)−Co | 117.85(13) |
| C(3)−N(3)−Co | 118.29(12) | C(5)−N(5)−Co | 117.91(12) |

Symmetry transformations used to generate equivalent atoms: **1**, (a) $-x, -y, -z$; **2**, (a) $-x, -y, -z$, (b) $-x, y, -z$; (c) $x, -y, z$; **3**, (a) $2 - x, -y, 2 - z$.

All hydrogen atoms were located in a difference Fourier map. They were refined with variable isotropic displacement parameters.

Due to low stability of the $Fe^{II}$ complex **2** in air, a crystal of dimensions $0.1 \times 0.1 \times 0.2$ mm was embedded in Araldite immediately after removal from the mother liquor. Data collection was performed on a Picker-Stoe four-circle diffractometer. An absorption correction was not applied. The structure was solved by direct methods of SHELXTL PLUS,[18] revealing all non-hydrogen atoms of the complex cation. All hydrogen atoms of the cation were located in a difference Fourier map. One of the two Cl atoms was located on a 2/*m* symmetry site. Three additional peaks in the asymmetric unit indicated the position of the second $Cl^-$ counterion and of additional water of crystallization. Since these remaining peaks were of comparable intensity, it was not possible to differentiate between Cl and O positions unambiguously. The assignment was therefore based on the interatomic distances to the closest neighbors. For O(1w) and O(2w), the values fell in the range of 2.76−2.88 Å, which is characteristic for hydrogen-bonded water molecules, whereas larger distances (2.93−3.29 Å) were found for Cl(2). Due to the observed electron density and in agreement with the charge balance, Cl(2) was refined with an occupancy of 0.5. All non-hydrogen atoms were refined in the anisotropic mode. Hydrogen atoms were included in the refinement with fixed coordinates as found in the difference Fourier map and with fixed isotropic displacement parameters of 0.05 $Å^2$.

Data for the two Co complexes **3** and **4** were collected on a Philips PW1100 four-circle diffractometer. An absorption correction was not performed. The structures were solved by direct methods using the computer program SDP86[20] and refined by full-matrix least-squares calculations on $F^2$ (SHELXL-93).[19] The hydrogen atoms of both

**Table 4.** Selected Bond Lengths (Å) and Angles (deg) of $[Co(taci)(Htaci)](NO_3)_4 \cdot 0.5H_2O$ (**4**), $[Co(taci)(tach)](NO_3)_3 \cdot 3H_2O$ (**5**), and $[Co(H_{-1}taci)(tach)](NO_3)_2 \cdot 2.8H_2O \cdot 0.2MeOH$ (**6**) with Esd's in Parentheses

| | | | |
|---|---|---|---|
| | $[Co(taci)(Htaci)](NO_3)_4 \cdot 0.5H_2O$ (**4**) | | |
| Co−O(22) | 1.984(3) | Co−O(24) | 1.893(3) |
| Co−N(11) | 1.924(4) | Co−N(13) | 1.954(4) |
| Co−N(15) | 1.943(4) | Co−N(23) | 1.960(4) |
| O(12)−C(12) | 1.423(7) | O(14)−C(14) | 1.422(6) |
| O(16)−C(16) | 1.422(7) | O(22)−C(22) | 1.460(5) |
| O(24)−C(24) | 1.421(6) | O(26)−C(26) | 1.424(6) |
| N(11)−C(11) | 1.479(6) | N(13)−C(13) | 1.481(6) |
| N(15)−C(15) | 1.479(6) | N(21)−C(21) | 1.476(6) |
| N(23)−C(23) | 1.482(5) | N(25)−C(25) | 1.492(6) |
| N(11)−Co−N(13) | 91.8(2) | N(11)−Co−N(15) | 90.1(2) |
| N(13)−Co−N(15) | 93.0(2) | N(11)−Co−O(22) | 174.7(2) |
| N(13)−Co−O(22) | 92.6(2) | N(15)−Co−O(22) | 92.6(2) |
| O(24)−Co−N(11) | 90.1(2) | O(24)−Co−N(13) | 178.1(2) |
| O(24)−Co−N(15) | 86.5(2) | O(24)−Co−N(23) | 85.8(2) |
| N(23)−Co−O(22) | 81.79(14) | O(24)−Co−O(22) | 85.5(2) |
| N(11)−Co−N(23) | 94.9(2) | N(13)−Co−N(23) | 94.4(2) |
| N(15)−Co−N(23) | 170.9(2) | C(22)−O(22)−Co | 110.5(3) |
| C(24)−O(24)−Co | 111.3(3) | C(11)−N(11)−Co | 118.7(3) |
| C(13)−N(13)−Co | 117.5(3) | C(15)−N(15)−Co | 118.6(3) |
| C(23)−N(23)−Co | 99.3(2) | | |
| | $[Co(taci)(tach)](NO_3)_3 \cdot 3H_2O$ (**5**) | | |
| Co−N(11) | 1.956(5) | Co−N(13) | 1.933(4) |
| Co−N(15) | 1.966(5) | Co−O(22) | 1.918(4) |
| Co−O(24) | 1.912(4) | Co−N(23) | 1.958(4) |
| O(22)−C(22) | 1.420(6) | O(24)−C(24) | 1.424(6) |
| O(26)−C(26) | 1.432(7) | N(11)−C(11) | 1.495(7) |
| N(13)−C(13) | 1.485(7) | N(15)−C(15) | 1.489(7) |
| N(21)−C(21) | 1.488(7) | N(23)−C(23) | 1.485(7) |
| N(25)−C(25) | 1.480(9) | | |
| N(11)−Co−N(13) | 91.1(2) | N(11)−Co−N(15) | 90.2(2) |
| N(13)−Co−N(15) | 92.6(2) | O(22)−Co−O(24) | 88.5(2) |
| O(22)−Co−N(23) | 84.1(2) | O(24)−Co−N(23) | 85.2(2) |
| N(11)−Co−N(23) | 94.9(2) | N(13)−Co−N(23) | 170.6(2) |
| N(15)−Co−N(23) | 94.6(2) | O(22)−Co−N(11) | 90.5(2) |
| O(22)−Co−N(13) | 88.6(2) | O(22)−Co−N(15) | 178.5(2) |
| O(24)−Co−N(11) | 179.0(2) | O(24)−Co−N(13) | 88.7(2) |
| O(24)−Co−N(15) | 90.8(2) | Co−N(11)−C(11) | 118.1(4) |
| Co−N(13)−C(13) | 119.6(3) | Co−N(15)−C(15) | 117.6(3) |
| Co−O(22)−C(22) | 110.4(3) | Co−O(24)−C(24) | 110.9(3) |
| Co−N(23)−C(23) | 97.9(3) | | |
| | $[Co(H_{-1}taci)(tach)](NO_3)_2 \cdot 2.8H_2O \cdot 0.2MeOH$ (**6**) | | |
| Co−N(11) | 1.947(3) | Co−N(13) | 1.962(3) |
| Co−N(15) | 1.955(3) | Co−O(24) | 1.887(2) |
| Co−N(23) | 1.983(3) | Co−N(25) | 1.977(3) |
| O(22)−C(22) | 1.424(4) | O(24)−C(24) | 1.404(4) |
| O(26)−C(26) | 1.437(4) | N(11)−C(11) | 1.484(5) |
| N(13)−C(13) | 1.488(4) | N(15)−C(15) | 1.489(4) |
| N(21)−C(21) | 1.468(5) | N(23)−C(23) | 1.501(4) |
| N(25)−C(25) | 1.496(4) | | |
| N(11)−Co−N(13) | 91.8(1) | N(11)−Co−N(15) | 90.2(1) |
| N(13)−Co−N(15) | 91.7(1) | O(24)−Co−N(23) | 84.5(1) |
| O(24)−Co−N(25) | 85.2(2) | N(23)−Co−N(25) | 84.6(2) |
| N(11)−Co−N(23) | 173.7(2) | N(13)−Co−N(23) | 94.0(2) |
| N(15)−Co−N(23) | 92.2(1) | O(24)−Co−N(11) | 89.7(1) |
| O(24)−Co−N(13) | 177.6(1) | O(24)−Co−N(15) | 90.2(2) |
| N(25)−Co−N(11) | 92.6(1) | N(25)−Co−N(13) | 92.8(2) |
| N(25)−Co−N(15) | 174.6(2) | Co−N(11)−C(11) | 119.1(2) |
| Co−N(13)−C(13) | 117.6(2) | Co−N(15)−C(15) | 118.8(2) |
| Co−O(24)−C(24) | 102.5(2) | Co−N(23)−C(23) | 108.0(2) |
| Co−N(25)−C(25) | 108.3(2) | | |

(18) Sheldrick, G. M. *SHELXTL-PLUS 88. Structure Determination Software Programs*; Nicolet Instrument Corp.: Madison, WI, 1988.
(19) Sheldrick, G. M.; *SHELXL-93. Program for the Refinement of Crystal Structures*, University of Göttingen: Göttingen, Germany.
(20) *SDP86 Structural Determination Package*; Enraf Nonius: Delft, The Netherlands, 1986.

complex cations could be located in a difference Fourier map. They were included in the refinement at calculated positions (riding model). Non-hydrogen atomic positions of **3** and **4** were all refined with anisotropic displacement parameters. There is some indication that the water position of **3** is not fully occupied. A partial occupancy of 0.75 would account for the rather large displacement parameter and for the observed amount of 1.5 equiv of $H_2O$ per Co, as required by the elemental analysis. In the structure of **4**, one of the four $NO_3^-$ counterions lies on a center of symmetry and is thus disordered. The oxygen positions of this disordered nitrate were refined with an occupancy of 0.5. However, a final difference Fourier synthesis still showed some remaining electron density around the disordered nitrate ion.

Data for the two $Co^{III}$−tach complexes **5** and **6** were collected on a Picker-Stoe four-circle diffractometer. A face indexed, numerical absorption corrections was applied to the data set of **5**. The two structures were solved using direct methods of SHELXTL PLUS.[18] All non-hydrogen atomic positions of **5** were refined in the anisotropic mode using full-matrix least-squares calculations of SHELXTL PLUS.[18] The hydrogen atoms of the complex cation and of one water molecule were located in a difference Fourier map and were refined with variable coordinates and variable isotropic displacement parameters. For **6**, the non-hydrogen atoms of the complex cation and of two water molecules could be located without difficulties; however, a difference Fourier synthesis showed additional electron density in vicinity of a center of symmetry at $^1/_2$, 0, $^1/_2$. In agreement with the elemental analysis and the NMR data, these peaks could be described as a superposition of randomly distributed $H_2O$ and MeOH molecules with occupancies of about 80% and 20%, respectively, having the oxygen position O(s) in common. In addition, the carbon atom of MeOH proved to be disordered. The structure was refined using anisotropic displacement parameters for all non-hydrogen atoms (SHELXL-93, full-matrix least-squares calculations on $F^2$).[19] Hydrogen atoms of the disordered solvent molecules were not considered. The hydrogen atoms of the two additional water molecules and of the noncoordinating amino group were located in the difference Fourier map and were refined with variable coordinates and variable isotropic displacement parameters. The remaining hydrogen positions were calculated (riding model) and included in the refinement with fixed isotropic displacement parameters.

## Results

**Preparation and Crystal Structure of $[M(taci)_2]^{2+}$ Complexes.** Crystalline solids of the $Mn^{II}$, $Fe^{II}$, and $Co^{II}$ complexes **1**−**3** can be obtained in reasonable yields by the simple combination of aqueous solutions of free taci and of the metal chlorides or nitrates. In solution, the complexes are rather sensitive to oxygen and they must therefore be prepared under an inert atmosphere. In the solid state, however, the Mn and Co complex are fairly stable and can be stored for several days without special protection. In contrast, the solid $Fe^{II}$ complex is rapidly oxidized upon exposure to air.

As shown previously, taci can bind a metal ion either in a symmetric (N−N−N or O−O−O coordination, $C_{3v}$ local symmetry)[3−6] or in an asymmetric manner (N−O−N or O−N−O, $C_s$ local symmetry; Chart 1).[21,22] The X-ray analyses of **1**−**3** established the presence of discrete, mononuclear bis-complexes in the solid state, with both ligands binding the metal center exclusively via their axial donor groups (symmetric coordination mode, Figure 1). The binding to the nitrogen donors ($MN_6$ coordination) was assigned on (a) the basis of the proper electron densities of N and O in the Fourier syntheses, (b) the comparison of C−O and C−N distances (Tables 3 and 4) which all fell in expected ranges, (c) the hydrogen atomic positions ($NH_2$ and OH) which could all be located in the difference Fourier map, forming a meaningful net of hydrogen bonds (Table 5), and (d) the observation that exchanging the O and N atoms resulted in a significant increase of the *R*-factors and in rather unusual displacement parameters. The $Mn^{II}$ complex **1** and the $Co^{II}$ complex **3** are isotypic with the previously reported $[Cd(taci)_2](NO_3)_2{\cdot}2H_2O$.[6] In this structure, the complex cations are linked to each other by hydrogen bonds of the type N−H···O. The structure is further stabilized by additional hydrogen bonds between the complex cations, the counterions, and the water of crystallization (Table 5). Similar N−H···O interactions between the complex cations are also found for the $Fe^{II}$ complex **2**. The metal atoms in **1**−**3** all lie on centers of inversion. Although there is no crystallographic 3-fold rotational symmetry, the deviation from $D_{3d}$ point symmetry for the three complexes is not significant and the coordination polyhedra can all be described as almost ideal trigonal antiprisma. There is, however, a significant deviation from octahedral coordination, which increases in the order **3** < **2** < **1**, as indicated by an increasing difference of the intramolecular and intermolecular N···N distances as well as a decrease of the intraligand and an increase of the interligand *cis*-N−M−N bond angles.

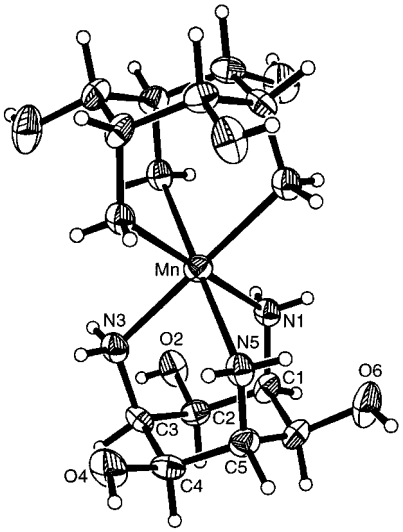


**Figure 1.** ORTEP representation of $[Mn(taci)_2]^{2+}$ (**1**) with numbering scheme and vibrational ellipsoids at the 50% probability level. Hydrogen atoms are shown as spheres of arbitrary size. The Fe complex **2** and the Co complex **3** adopt the same structure.

**Table 5.** Interatomic Distances [*d* (Å)] and Angles [α (deg)] of the Hydrogen Bonds in the Crystal Structure of $[Mn(taci)_2](NO_3)_2{\cdot}2H_2O$ (**1**) with Esd's in Parentheses

| X−H···Y | *d*(X−H) | *d*(H···Y) | *d*(X···Y) | α(X−H···Y) |
|---|---|---|---|---|
| N(1)−H(11)···O(11) | 0.87(2) | 2.28(2) | 3.107(2) | 159(2) |
| N(1)−H(12)···O(1W) | 0.87(2) | 2.37(2) | 3.193(2) | 158(2) |
| O(2)−H(21)···O(31) | 0.73(2) | 2.15(2) | 2.849(2) | 159(2) |
| N(3)−H(31)···O(2) | 0.91(2) | 2.31(2) | 3.137(2) | 151(2) |
| N(3)−H(32)···O(11) | 0.85(2) | 2.33(2) | 3.124(2) | 157(2) |
| O(4)−H(41)···O(11) | 0.77(3) | 2.11(3) | 2.848(2) | 162(3) |
| N(5)−H(51)···O(2) | 0.85(2) | 2.19(2) | 3.023(2) | 167(2) |
| N(5)−H(52)···O(1W) | 0.84(2) | 2.34(2) | 3.156(3) | 164(2) |
| O(6)−H(61)···O(21) | 0.69(2) | 2.19(2) | 2.828(3) | 153(3) |
| O(1W)−H(1W)···O(4) | 0.74(3) | 2.10(3) | 2.828(2) | 171(3) |
| O(1W)−H(2W)···O(1W) | 0.53(6) | 2.56(5) | 2.984(4) | 141(7) |

**EPR Spectroscopy and Magnetic Measurements.** The EPR spectra of the $Mn^{II}$−taci complex **1** in slightly alkaline aqueous solution (pH 7.9) showed the expected 6-line signal ($g = 2.02 \pm 0.02$, width of signal = 650 G) indicating the presence of a high-spin ($S = {}^5/_2$) $Mn^{II}$ species. As the pH of the solution was increased, there was a rapid decrease in the

(21) Hegetschweiler, K.; Ghisletta, M.; Gramlich, V. *Inorg. Chem.* **1993**, *32*, 2699.
(22) Hegetschweiler, K.; Wörle, M.; Meienberger, M. D.; Nesper, R.; Schmalle, H. W.; Hancock, R. D. *Inorg. Chim. Acta* **1996**, *250*, 35.

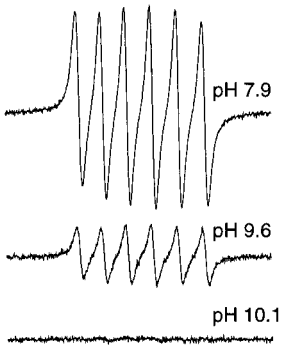


**Figure 2.** EPR spectra of the $Mn^{II}$−taci complex (total [Mn] = $2.4 \times 10^{-3}$; total [taci] = $1.4 \times 10^{-2}$ M) at different pH values as indicated.

**Table 6.** Survey of Stability Constants (25 °C, 0.1 M $KNO_3$, $K_1 = [ML][M]^{-1}[L]^{-1}$, $K_2 = [ML_2][ML]^{-1}[L]^{-1}$) of taci (L) Complexes with Divalent Metal Ions with Esd's Given in Parentheses

| $M^{II}$ | log $K_1$ | log $K_2$ |
|---|---|---|
| Mn | 4.0(1)[a] | <3 |
| Fe | 6.40(3) | 4.78(3) |
| Co | 9.10(1) | 6.58(1) |
| Ni[b] | 12.37(1) | 8.57(1) |
| Cu[b] | 12.09(1) | 6.70(1) |
| Zn[b] | 8.40(1) | 5.16(1) |
| Cd[c] | 6.48(3) | 4.47(3) |

[a] 1 M $KNO_3$. [b] Data from ref 3. [c] Data from ref 6.

intensity of this signal (Figure 2). It finally disappeared completely at pH 10, and the sample remained EPR-silent at higher pH. Solutions of the $Mn^{IV}$ complex, which were obtained by oxygenation of an $Mn^{II}$ sample at pH = 11 were also EPR-silent.

The magnetic susceptibility measurements of the solid $Mn^{II}$ complex **1** exhibited no significant deviation from the Curie law in the range 1.7−300 K. A least-squares analysis revealed a temperature-independent magnetic moment $\mu$ of 5.9 $\mu_B$, confirming the presence of a high-spin $d^5$ electron configuration. In the range 90−400 K, the magnetic susceptibility of the solid dehydrated $Fe^{II}$ complex **2** obeyed Curie−Weiss behavior with $\Theta$ = 10 K. The magnetic moment at 25 °C was found to be 5.45 $\mu_B$, indicating that $Fe^{II}$ was present in the high-spin $d^6$ electron configuration with a significant orbit contribution.

**Determination of Stability Constants.** A series of potentiometric titrations was performed to establish the stability of the taci complexes with the divalent metal cations in aqueous media (0.1 $KNO_3$, 25 °C). Standardized KOH or $HNO_3$ was added to solutions of $H_3taci^{3+}$ or taci, respectively, and the pH was recorded in the presence and absence of the metal ions (Figure 3). Corresponding experiments with $Ni^{II}$, $Cu^{II}$, $Zn^{II}$, and $Cd^{II}$ have been reported previously[3,6] and are included in Figure 3 for comparison. In the range $0 < a < 3$ ($a$ = equiv of titrant added/equiv of total taci), the presence of the metal cations caused a decrease in pH, indicating complex formation. This effect is most dominant for $Ni^{II}$ and $Cu^{II}$ but barely significant for $Mn^{II}$. Obviously, the complex stability increases dramatically in the order $Mn^{II} \ll Cd^{II} \approx Fe^{II} < Zn^{II} < Co^{II} < Cu^{II} < Ni^{II}$. In particular, significant amounts of the $Mn^{II}$ complex do not form below pH 7. With the sole exception of $Mn^{II}$, the titration experiments with [M]:[taci] = 1:2 were evaluated by considering the formation of $[M(taci)]^{2+}$ and $[M(taci)_2]^{2+}$ (Table 6). The formation constants of the 1:1 complexes were also determined by titration experiments with a ratio of [M]:[taci] = 1:1. The two types of titrations did not reveal any significant differences for the stability constants of

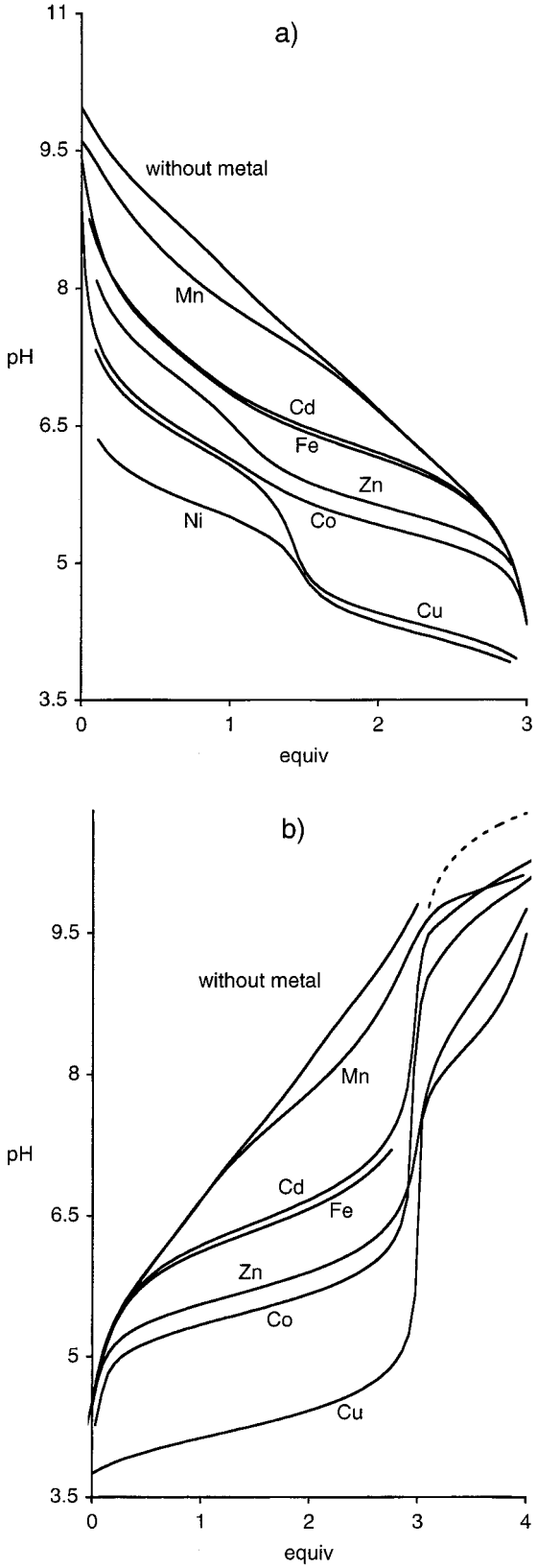


**Figure 3.** Titration curves (25 °C, 0.1 M $KNO_3$) of taci in the presence and absence of divalent metal cations as indicated (equiv = equivalents of titrant added/equiv of taci). The data for Ni, Cu, Zn, and Cd are taken from refs 3 and 6. (a) Addition of $HNO_3$ (0.1 M) to solutions with a total taci concentration of $2 \times 10^{-3}$ M and a total metal concentration (if present) of $10^{-3}$ M. (b) Addition of KOH (0.1 M) to solutions of taci·$3HNO_3$ (total taci concentration = $10^{-3}$ M) and (if present) a metal salt with a total metal concentration of $10^{-3}$ M. The dotted line is calculated for a system where no additional $OH^-$ is consumed after the formation of $[M(taci)]^{2+}$.

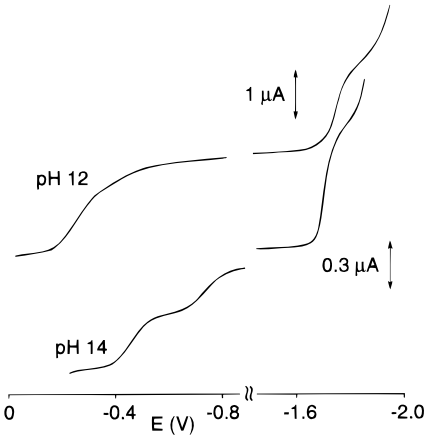


**Figure 4.** Polarograms of the Mn complex **1**. The potential is measured versus the saturated calomel reference electrode (SCE).

**Table 7.** Polarographic Data for Mn−taci Complexes (Total [Mn] = $1.22 \times 10^{-3}$ M, Total [taci] = $4.87 \times 10^{-3}$ M), with Potentials Quoted versus the Saturated Calomel Reference Electrode (SCE)

| electrode process | $E_{1/2}$ (V)[a] | $i_d$ ($\mu$A) | $\alpha$[a] | pH |
|---|---|---|---|---|
| $Mn^{II} \rightarrow Mn^{IV}$ | −0.27 | 2.35 | 0.35 | 12 |
| $Mn^{II} \rightarrow Mn^{0}$ | −1.75 | 2.25 | 0.94 | 12 |
| $Mn^{IV} \rightarrow Mn^{III}$ [b] | −0.29 | 1.28 | 1.02 | 12 |
| $Mn^{III} \rightarrow Mn^{II}$ [b] | −0.71 | 2.56 | 0.25 | 12 |
| $Mn^{II} \rightarrow Mn^{0}$ [b] | −1.76 | 3.74 | 1.05 | 12 |
| $Mn^{II} \rightarrow Mn^{III}$ | −0.75 | 0.43 | 0.59 | 14 |
| $Mn^{III} \rightarrow Mn^{IV}$ | −0.48 | 0.53 | 0.94 | 14 |
| $Mn^{II} \rightarrow Mn^{0}$ | −1.75 | 1.10 | 1.06 | 14 |
| $Mn^{IV} \rightarrow Mn^{III}$ [b] | −0.49 | 4.75 | 1.01 | 14 |
| $Mn^{III} \rightarrow Mn^{II}$ [b] | −0.73 | 2.88 | 0.91 | 14 |
| $Mn^{II} \rightarrow Mn^{0}$ [b] | −1.75 | 3.47 | 1.02 | 14 |

[a] The estimated standard deviations are 0.003 V for $E_{1/2}$ and 0.02 for $\alpha$. [b] A sample of a $Mn^{IV}$ complex, prepared in situ by oxidation with dioxygen, was used as starting material.

$[M(taci)]^{2+}$; however, the latter experiment provided evidence for the additional formation of the deprotonated complexes $[H_{-n}M_x(taci)_y]^{2x-n}$ at high pH. This is indicated by the appearance of a second buffer region at $a > 3$. For $Cu^{II}$ and $Zn^{II}$, the formation of such deprotonated species occurred at significantly lower pH than for $Co^{II}$, $Fe^{II}$, $Cd^{II}$, and $Mn^{II}$. It was, however, not possible to identify unambiguously the precise composition or the nuclearity of the species formed, and this part of the titration curve was therefore not used in the evaluation of the stability constants. Due to the low stability of the $Mn^{II}$−taci complexes, additional titrations were carried out with a total taci concentration of $10^{-2}$ M. Under these conditions (25 °C, 1 M $KNO_3$), $[Mn(taci)]^{2+}$ forms to a sufficient extent in the range $7 < pH < 8$ to allow the evaluation of the formation constant $K_1 = [Mn(taci)^{2+}][Mn^{2+}]^{-1}[taci]^{-1}$, $\log K_1 = 4.0(1)$.

**Electrochemistry.** The redox properties of the Mn−taci system in alkaline aqueous solutions was investigated by polarographic measurements (Figure 4). The results are summarized in Table 7. The free ligand itself cannot be reduced or oxidized at a dropping mercury electrode. One cathodic and one anodic wave of approximately the same height appeared in the presence of $Mn^{II}$ and excess taci at pH 12. Both waves correspond to two-electron processes, which was checked by controlled potential electrolysis, yielding a number of 2.04 and 1.98 exchanged electrons, respectively. The reduction wave was assigned to the reversible formation of elemental Mn, whereas the oxidation wave indicated the irreversible formation of a $Mn^{IV}$ complex. At pH 14, the oxidation wave splits into two separate steps, indicating the formation of a $Mn^{III}$ intermediate. The second oxidation wave and the reduction wave proved to be reversible, while the first oxidation wave was irreversible. In alkaline medium, the $Mn^{II}$−taci complex can be oxidized by dioxygen to the $Mn^{IV}$ species. The polarograms recorded after oxidation showed three reduction waves corresponding to the final formation of $Mn^0$ with $Mn^{III}$ and $Mn^{II}$ as intermediates.

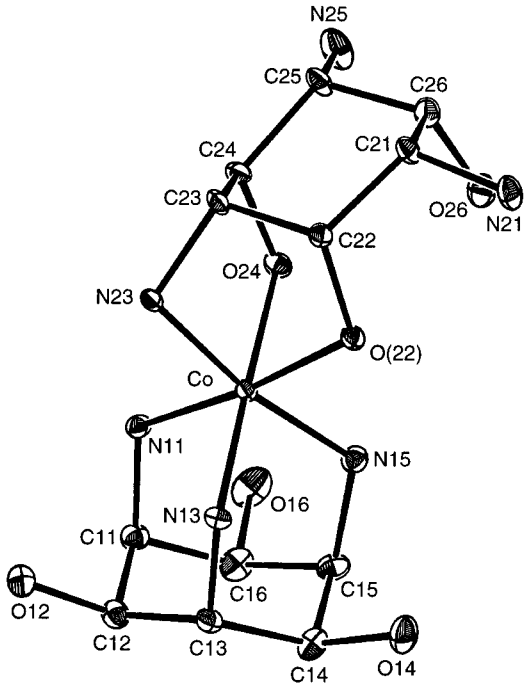


**Figure 5.** Structural diagram of $[Co(taci)(Htaci)]^{4+}$ (**4**) with numbering scheme. The hydrogen atoms are omitted, and the displacement ellipsoids are shown at the 30% probability level for clarity.

The redox properties of the Fe−taci and the Co−taci systems were investigated by cyclic voltammetry in alkaline aqueous solution (pH 9.5). Starting with the divalent metal cations, both complexes showed quasi reversible redox behavior with estimated redox potentials of +0.09 V (Fe) and −0.37 V (Co) versus the standard hydrogen electrode (SHE). For both complexes, a significant increase of the peak to peak separation was observed with increasing scan rate. Extrapolation to scan rate 0 revealed a separation of 79 ± 2 mV for the Fe complex and 67 ± 3 mV for the Co complex. In both cases, the peak currents showed the expected square root dependence on the scan rate, indicating a diffusion-controlled process.

**Preparation and Structure of the $Co^{III}$ Complexes 4−6.** The bis-taci complex **4** was obtained by a one-pot reaction using an excess of $Co^{II}$. The two mixed $Co^{III}$−tach−taci complexes **5** and **6** were prepared by a two-step procedure with Co(tach)-$(NO_3)_3$ as intermediate. All three complexes have structures, with one taci ligand present in an "asymmetric" type-ii or type-iii coordination mode (Figures 5 and 6). In the bis-taci complex **4**, one of the taci ligands binds the $Co^{III}$ center by the three amino groups, whereas the second ligand is coordinated via one nitrogen and two oxygen donors. The presence of a *cis*-$CoN_4O_2$ chromophore[23] is indicated by the vis spectrum ($\lambda_{max} = 494$ nm, $\epsilon = 86\ M^{-1}\ cm^{-1}$). Both $^1H$ and $^{13}C$ NMR spectroscopies show 8 resonances, as expected for $C_s$ point symmetry, and the peaks could be fully assigned by a $^1H-^1H$ COSY experiment (Figure 7). The crystal structure showed the presence of four $NO_3^-$ counterions per complex cation, as indicated by elemental analysis. Obviously, the asymmetric ligand coordinates in a

(23) Basolo, F. *J. Am. Chem. Soc.* **1950**, *72*, 4393.

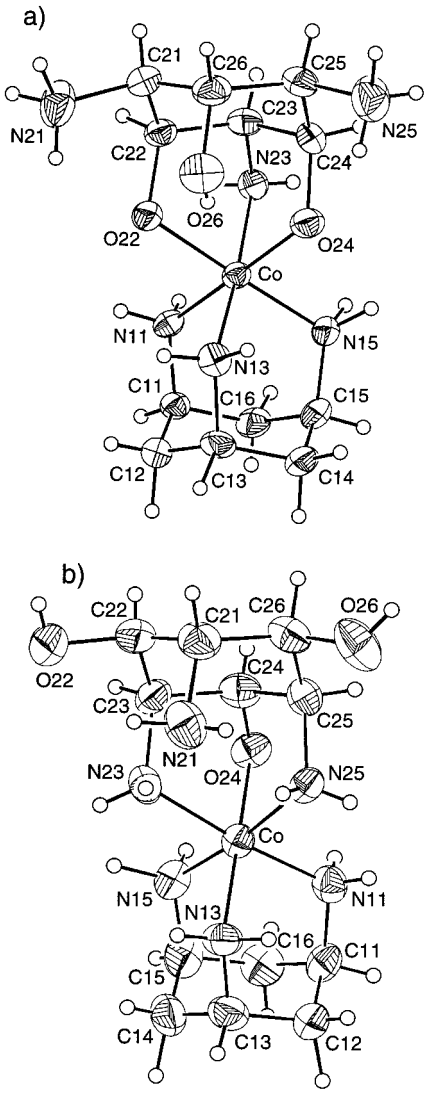


**Figure 6.** Structural diagrams of a) $[Co(tach)(taci)]^{3+}$ (**5**) and b) $[Co(tach)(H_{-1}taci)]^{2+}$ (**6**) with numbering scheme. The displacement ellipsoids are shown at the 50% probability level. The hydrogen atoms are shown as spheres of arbitrary size.

protonated form as $Htaci^{+}$. This is not surprising, since the compound was isolated from acidic aqueous solution. On the basis of the significant differences for the Co−O bond distances of 1.984(3) and 1.891(3) Å, it can be concluded that one of the two oxygen donors is deprotonated. In agreement with this interpretation, a difference Fourier map showed additional electron density in proximity to O(22) assignable to the expected H(−O) atom. In addition, the noncoordinating nitrogen donors are both protonated. The coordination of one hydroxo and one alkoxo group lowers the symmetry to $C_1$, but the observed symmetry in aqueous solution remains $C_s$ even under acidic conditions because of the fast proton exchange. Moreover, complex **4** behaves as a strong acid and deprotonation of the coordinated hydroxy group occurs above pH 3.

The mixed tach−taci complex **5** ($\lambda_{max} = 498$ nm, $\epsilon = 76$ $M^{-1}$ $cm^{-1}$) has essentially the same structure as the bis−taci complex **4**. However, complex **5** was crystallized under neutral conditions and, consequently, protonation of a coordinated oxygen donor was not observed in the crystal structure. The $^{1}H$ and $^{13}C$ NMR spectra of complexes **4** and **5** showed no significant differences for the asymmetrically bound taci ligand. The chemical shifts revealed a characteristic pH dependence in the range $1 < pD < 3$ and $7 < pD < 11$ (Figure 7c). At pD

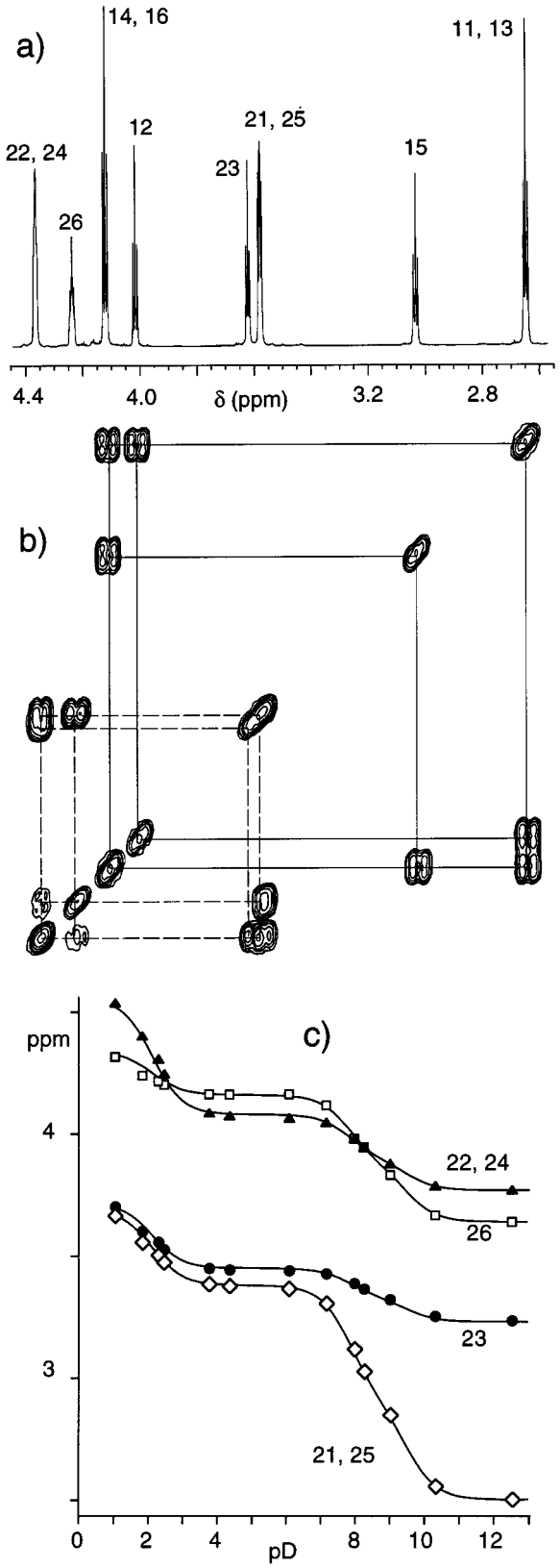


**Figure 7.** NMR data for the two $Co^{III}$ complexes **4** and **5**, adopting type iii structures: (a) $^{1}H$ spectrum of **4** with assignment of signals; (b) the corresponding $^{1}H-^{1}H$ COSY; (c) pH dependence of some $^{1}H$ resonances of **5**. The points correspond to experimental values. The solid lines were calculated by a least-squares procedure as described in ref 12, assuming an equilibrium between the four species $[Co(tach)(Htaci)]^{4+}$, $[Co(tach)(taci)]^{3+}$, $[Co(tach)(H_{-1}taci)]^{2+}$, and $[Co(tach)(H_{-2}taci)]^{+}$. The calculations were performed by refining the 3 $pK_a$ values and the chemical shifts of these four species. The numbering scheme corresponds to the crystal structures (Figures 5 and 6a).

7, this ligand is present as a neutral zwitterion with two deprotonated oxygen donors and two protonated nitrogen donors. At higher pH, successive deprotonation of the ammonium groups occurs, with the monopositive $[CoL(H_{-2}taci)]^+$ being formed above pD 11 (L = tach or the symmetrically bound taci). The pD dependence in the acidic range originates from the above-mentioned protonation of a coordinated oxygen donor resulting in the formation of $[CoL(Htaci)]^{4+}$. In agreement with our assignments, the most pronounced chemical shifts are found for H(22) and H(24) in the acidic region and for H(21) and H(25) in the alkaline region. Corresponding p$K_a$ values of 2.0-(2), 7.23(1), and 8.84(1) were established by potentiometric titrations (0.1 M $KNO_3$, 25 °C).

The $^1$H and $^{13}$C NMR data of complex **6** also indicate an asymmetric coordination mode of the taci ligand, and in accordance with $C_s$ point symmetry, four resonances are found in the spectra in a 1:2:2:1 ratio. However, the vis spectrum with maxima at 379 nm ($\epsilon$ = 136 $M^{-1}$ $cm^{-1}$) and 484 nm ($\epsilon$ = 64 $M^{-1}$ $cm^{-1}$) is indicative of a $CoN_5O$ chromophore.[23,24] Such a coordination mode requires a type ii structure with Co bound to one equatorial oxygen and two axial nitrogen donors. This structural assignment was confirmed by X-ray analysis (Figure 6b). It is noteworthy that the complex is present in the deprotonated form $[Co(taci)(H_{-1}taci)]^{2+}$ even under acidic conditions. Obviously, it is not possible to protonate the third axial amino group. Using molecular mechanics, we recently showed that, in the zwitterionic form of the type ii coordination mode, there would be substantial repulsion between the H(−N) hydrogen atoms.[22] This repulsive interaction was overlooked in the first contribution of this series,[3] where this structure type was postulated for $[HCu(taci)_2]^{3+}$, which was observed as a minor species in the titration of $[Cu(taci)_2]^{2+}$. Type ii coordination is only possible if the structure is stabilized by 1,3-diaxial N−H···N bonds.[25] The necessity of such hydrogen bonds has recently been demonstrated for a related Re(V) complex with an alkylated taci derivative exhibiting type ii coordination.[26] However, after suppression of the possibility of 1,3 N−H···N interactions by converting the noncoordinating amino group into the corresponding amide, the breakdown of the hydrogen bonds resulted in a characteristic structural rearrangement with the cyclohexane ring adopting a twisted boat rather than a chair conformation.

## Discussion

**Crystal Structures of $[M(taci)_2]^{2+}$.** In the previous contributions, we reported the structure of bis-taci complexes with the divalent metal cations $Ni^{II}$, $Cu^{II}$, $Zn^{II}$, and $Cd^{II}$.[3,6] In addition, the steric demands of taci were analyzed by means of molecular mechanics calculations.[6,22] In the present paper, the data for $Mn^{II}$, $Co^{II}$, and $Fe^{II}$ are added to this series. These results now allow a comprehensive discussion of structural parameters for divalent transition- and $d^{10}$-metal cations. In the solid state, all these metal ions form bis complexes $[M(taci)_2]^{2+}$ with $MN_6$ coordination. A systematic inspection of the structural parameters as a function of metal ion size[27] reveals (i) a strictly linear increase of the mean M−N bond lengths, (ii) a decrease of the intraligand N−M−N bond angles (and as a consequence an increase of the interligand N−M−N bond angles), and (iii) increasing interligand (and to a lesser extent intraligand) N···N distances (Figure 8). These properties are in agreement with the elongation of the $MN_6$ core along the pseudotrigonal axis.[28] A similar relationship has previously been observed between the structural parameters of bis-taci complexes with an $MO_6$ coordination. It is interesting, however, that there is no obvious correlation between the C−N−M bond angle and the metal ion size. This is in contrast to the $MO_6$ structures, where a significant widening of the C−O−M angle was observed for the larger metal ions.[6]

**Structures of the $Co^{III}$ Complexes 4−6.** In the preceding section, the structural characterization of a variety of complexes with a bis-type i coordination was used to analyze systematic changes of this coordination mode as a function of metal ion size. The structure analyses of the three $Co^{III}$ complexes **4**−**6** on the other hand allows the first direct comparison of three different coordination modes of taci with the same metal cation (Table 4). In contrast to the well-known symmetric ($CoN_3$) type i coordination, the asymmetric type ii and type iii coordination modes cause some characteristic distortion of the ligand framework. This becomes evident when comparing nonbonding intraligand interactions between the substituents in a 1,2-axial−equatorial and a 1,3-diaxial arrangement. For symmetric type i coordination such as that found for the N,N,N-bonded taci ligand of **4** and for the previously reported bis-type i isomer of $[Co(taci)_2]^{3+}$,[4] there is no significant difference between the two types of distances. They both fall in the range 2.73−2.85 Å, in close agreement with the values observed for the free ligand.[6] However, in the asymmetrically bound ligands of **4**−**6**, the distances between the coordinated donor atoms with an 1,2-axial−equatorial arrangement all lie between 2.59 and 2.62 Å. This is remarkably short and indicates considerable strain for these coordination modes. Strain is also indicated by the rather small $C-N_{eq}-Co$ and $C-O_{eq}-Co$ angles (98.0−102.5°). Molecular mechanics calculations showed that the coordination of a small metal ion such as $Co^{III}$ to the 1,3,5-triaxial donor set of taci results in almost strain-free structures, whereas binding to the asymmetric 1,2,3-axial−equatorial−axial arrangement of the donor set is less favorable.[22,29]

**Species in Aqueous Solution.** The formation of $[M(taci)]^{2+}$ and $[M(taci)_2]^{2+}$ for M = Fe and Co is well established. By contrast, only weak interactions are observed for $Mn^{II}$. The low stability of $Mn^{II}$−taci complexes results from the strain induced by the rather large size of this metal ion[6] and from its electronic structure (high-spin $d^5$ configuration without any ligand field stabilization). Obviously, $[Mn(taci)_2]^{2+}$ dissociates in dilute aqueous solution and the ready formation of solid $[Mn(taci)_2](NO_3)_2 \cdot 2H_2O$ must be discussed in terms of a particularly favorable lattice energy. Below pH 7.5 the protonation of the ligand overrides the formation of a bis complex, while at higher pH a competitive reaction of $OH^-$ with $[Mn(taci)]^{2+}$ must be taken into consideration. The potentiometric measurements indeed confirmed the formation of the 1:1 complex $[Mn(taci)]^{2+}$ at pH 7−8. In addition, they showed that species of the tentative composition $[H_{-n}Mn_x(taci)_y(OH)_m]^{2x-n-m}$ ($y < 2x$) form preferentially at high pH. The formation of *polynuclear* complexes

(24) Alexander, M. D.; Spillert, C. A. *Inorg. Chem.* **1970**, *9*, 2344.
(25) Liang, C.; Ewig, C. S.; Stouch, T. R.; Hagler, A. T. *J. Am. Chem. Soc.* **1994**, *116*, 3904.
(26) Kramer, A.; Alberto, R.; Egli, A.; Novak-Hofer, I.; Hegetschweiler, K.; Abram, U.; Bernhardt, P. V.; Schubiger, P. A. Submitted.
(27) Shannon, R. D. *Acta Crystallogr.* **1976**, *A32*, 751.
(28) Hegetschweiler, K.; Kradolfer, T.; Gramlich, V.; Hancock, R. D. *Chem. Eur. J.* **1995**, *1*, 74.
(29) It should, however, be noted that in a 1:2 complex, having a bis-type i structure, additional interligand repulsion between coordinated $NH_2$ groups leads to considerable strain for small metal cations such as $Co^{III}$ (see ref 6). This type of repulsion is apparently less significant for the type i−ii and type i−iii structures, as demonstrated by the mean Co−N bond distances for the type i taci ligand, which is 1.94 Å for **4** but 2.00 Å for the bis-type i complex (ref 4).

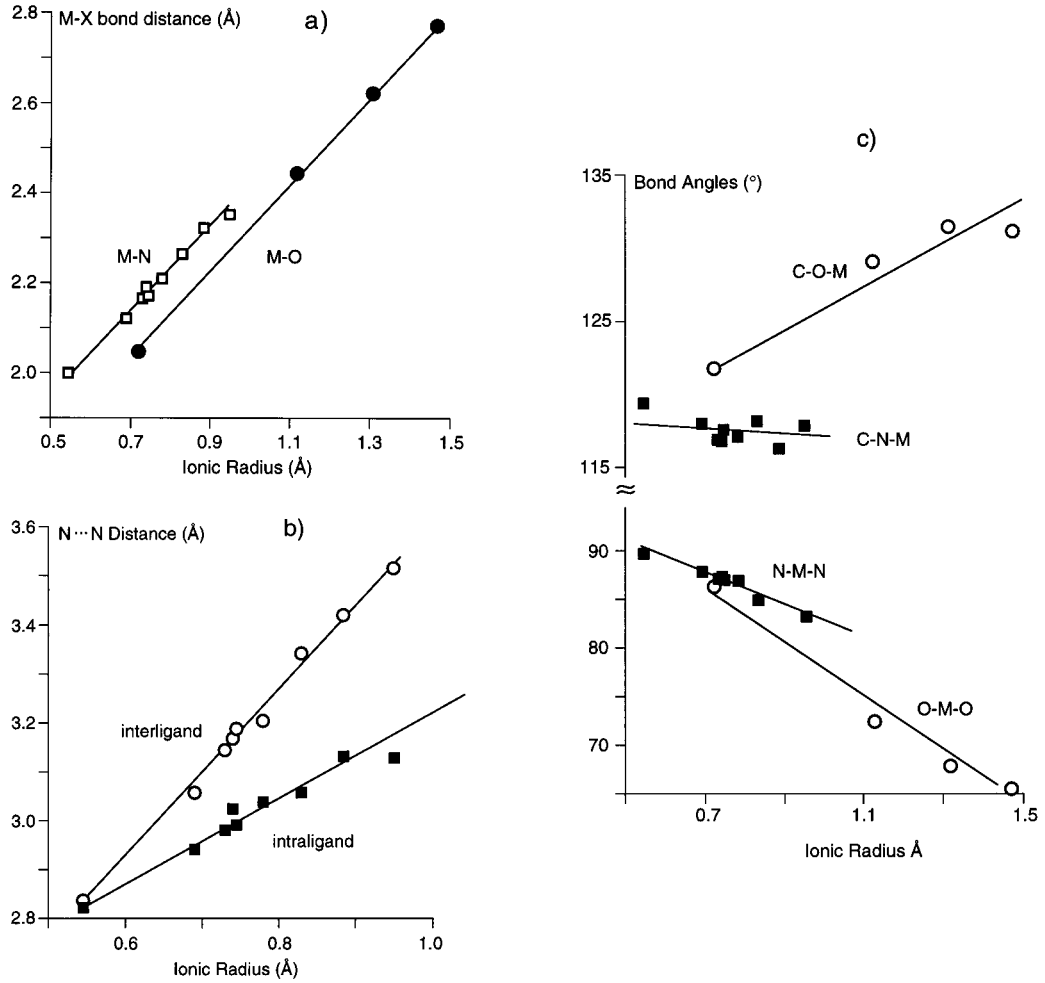


**Figure 8.** Synopsis of structural parameters for bis-type i and bis-type iv coordination: (a) mean M−N and M−O bond distances; (b) mean intraligand N···N and mean interligand *cis*-N···N distances in bis-type i complexes; (c) mean N−M−N, O−M−O, C−O−M, and C−N−M bond angles. The complexes of $Mn^{II}$, $Co^{II}$, $Co^{III}$, $Ni^{II}$, $Cu^{II}$, $Zn^{II}$, and $Cd^{II}$ were considered for the bis-type i structure (data from this work and from refs 3, 4, and 6). The data for the complexes with bis-type iv structures (Mg, Ca, Sr, and Ba complexes) are from ref 6. Mean structural parameters are shown as individual points; the solid lines visualize trends of these data and do not correspond to any experimental quantities.

($x \geq 2$) is strongly supported by the EPR data (Figure 2). The six-line pattern observed at pH 7.9 is indicative of mononuclear high-spin $Mn^{II}$. Analogous spectra have been observed for many $Mn^{II}$ salt solutions of similar concentrations in the presence of D-saccharose, D-gluconate, or maltitol.[30] The disappearance of the signal with increasing pH is indicative of antiferromagnetic coupling, which means that hydroxo- or alkoxo-bridged species are probably formed. In the past, such polynuclear species were formulated as hydroxo-bridged complexes ($m > 0$); however, recent investigations have established that coordinated alkoxo groups of a polyol ligand also have a pronounced tendency for such bridging interactions.[31,32] The exclusive coordination of the divalent $d^{10}$ and transition metal centers to nitrogen donors in the bis complexes must thus be attributed to the rather poor donor capacity of the (uncharged) hydroxy groups, and the coordination mode may well change at high pH. In fact, the oxygen donors of taci are only effective in metal binding if they are deprotonated.[28] For the $Co^{III}$ complex **5**, coordination to alkoxo groups is even possible in acidic media, since the noncoordinated amino groups act as an *internal* base, facilitating the deprotonation of the oxygen donors and generating a zwitterionic form of taci. However, it has recently been shown that, in the case of the divalent $Mg^{2+}$, $Ca^{2+}$, $Sr^{2+}$, and $Ba^{2+}$, the coordinated hydroxy groups are not sufficiently acidic to cause such a proton transfer from O to N and they remain protonated.[6] The divalent $Mn^{2+}$, $Fe^{2+}$, and $Co^{2+}$ are only slightly stronger acids than $Mg^{2+}$,[8] and a noncoordinating amino group in such a complex would probably not be sufficiently basic to abstract a proton from a coordinated hydroxy group. However, in the high-pH region, where the formation of the polynuclear complexes is observed, a sufficient amount of $OH^-$ (a much stronger *external* base) is now operative and the deprotonation of the hydroxy group can readily occur.

**Redox Chemistry.** The present study established that the $Mn^{II}$, $Fe^{II}$, and $Co^{II}$ taci complexes that are formed in alkaline aqueous media readily undergo metal-centered oxidation. This reaction is, however, rather complex, since different coordination modes of taci must be considered for the different oxidation states of the metal center. For Mn, our results do not allow any structural assignments of the intermediate $Mn^{III}$ or the final $Mn^{IV}$ complex. For the $Fe^{II}$ hexaamine complex **2**, the magnetic

(30) (a) Nagy, L.; Gajda, T.; Burger, K.; Pali, T. *Inorg. Chim. Acta* **1986**, *123*, 35. (b) Nagy, L.; Gajda, T.; Pali, T.; Burger, K. *Acta Chim. Hung.* **1988**, *125*, 403. (c) Bodini, M. E.; Willis, L. A.; Riechel, T. L.; Sawyer, D. T. *Inorg. Chem.* **1976**, *15*, 1538. (d) Rocha, C.; Ferreira, A. M. Da C. *Int. J. Chem. Kinet.* **1994**, *26*, 1121.

(31) Hegetschweiler, K.; Hausherr-Primo, L.; Koppenol, W. H.; Gramlich, V.; Odier, L.; Meyer, W.; Winkler, H.; Trautwein, A. X. *Angew. Chem., Int. Ed. Engl.* **1995**, *34*, 2242.

(32) (a) Hegetschweiler, K.; Ghisletta, M.; Fässler, T. F.; Nesper, R. *Angew. Chem., Int. Ed. Engl.* **1993**, *32*, 1426. (b) Burger, J.; Gack, C.; Klüfers, P. *Angew. Chem., Int. Ed. Engl.* **1995**, *34*, 2647.

susceptibility measurements established a high-spin electron configuration. It is, however, to be expected that the corresponding $Fe^{III}$ complex with the same $FeN_6$ coordination would be low spin, by analogy with the formation of the low-spin, hexaamine complex $[Fe(tmca)_2]^{3+}$ (tmca = *all-cis*-2,4,6-trimethoxycyclohexane-1,3,5-triamine is a tris O-methylated derivative of taci).[33] On the other hand, a type i−iv coordination has recently been established for the stable form of the bis−taci complex of $Fe^{III}$.[34] If one assumes that in both oxidation stages the reacting species correspond to the most stable forms of the bis complexes, a structural rearrangement from a bis-type i structure for $Fe^{II}$ to a type i−iv structure for $Fe^{III}$ is required to take place during the reaction. It has previously been noted that the low-spin $[Fe(tmca)_2]^{3+}$ complex proved to be inert with respect to ligand substitution. It is thus rather unlikely that this rearrangement occurs at the trivalent stage.

The $Co^{II}/Co^{III}$−taci system behaves similarly in the respect that the divalent complexes are generally labile, whereas the hexaamine $[Co(taci)_2]^{3+}$ is inert. However, in contrast to $Fe^{III}$, all known isomers of the $Co^{III}$−taci complexes are diamagnetic and, due to the inertness of the low-spin $Co^{III}$−N bond, the different isomers can be isolated and their structures can be analyzed. This induced us to perform a case study by elucidating the product distribution and the structural properties of a variety of $Co^{III}$−taci complexes as a function of the specific reaction conditions. Such complexes may be formed either by oxidation of the corresponding $Co^{II}$ precursor or by substitution of rather labile ligands at $Co^{III}$. $[Co^{II}(taci)_2]^{2+}$ forms almost quantitatively in alkaline aqueous solution upon addition of $Co^{2+}$ to taci in a 1:2 molar ratio. This complex can be oxidized to the hexaamine $Co^{III}$ complex by the usual procedure using dioxygen as oxidizing agent.[4] It is noteworthy that the addition of a second portion of $Co^{2+}$ to the reaction mixture resulted in the formation of a significant amount of the bis-complex **4**, where one of the taci ligands is bound by one nitrogen and two oxygen atoms. It was, however, difficult, to reproduce this result by following the preparation procedure, given in the Experimental Section. Repetition of this protocol frequently resulted in the formation of the symmetric bis-type i isomer with the hexaamine coordination. Obviously, minimal changes of the reaction conditions had a significant influence on product distribution. It is clear that the two different isomers must form by different mechanisms of the oxidation reaction; rearrangement of a coordinated taci ligand at the trivalent state of Co can be excluded. To elucidate the mechanism by which complex **4** is formed, we prepared $[Co(tach)(H_2O)_x(NO_3)_{3-x}]^{x+}$ ($0 \le x \le 3$) as a suitable model and investigated the reaction of this complex with taci. The tach ligand was chosen since this molecule contains no hydroxy groups and coordination can only occur through the three nitrogen atoms. A series of well-reproducible substitution experiments was performed, yielding substantial amounts of the two asymmetric isomers **5** and **6** (Scheme 1). There was, however, no sign of the symmetric hexaamine isomer. If one assumes initial binding of only one of the primary amino groups of the entering taci to the Co(tach) moiety, the formation of the asymmetric complexes becomes understandable. It is well-known that the coordination of subsequent primary amino groups of polyamine ligands to $Co^{III}$ may occur at a rather low rate in aqueous solution. For example, the reaction of *trans*-$[Co(en)_2Cl_2]Cl$ with en (=1,2-diaminoethane) in MeOH resulted in the formation of *cis*-$[Co(en)_2(Hen\text{-}\kappa N)Cl]Cl_3$ and the subsequent reaction in $H_2O$ at pH 8.5 resulted in the formation of *cis*-$[Co(en)_2(en\text{-}\kappa N)(OH)]^{2+}$.[24] Rapid formation of the hexaamine $[Co(en)_3]^{3+}$ was not observed. The present investigation thus provides evidence that, after oxidation, re-entry of a partially or completely dissociated taci ligand would result in the formation of an asymmetric complex such as **4** (where the re-entering ligand has a type ii or type iii structure), whereas the symmetric bis-type i isomer will only form by the direct oxidation of the corresponding $Co^{II}$ precursor.

The observation of the asymmetric coordination modes in **4**−**6** could also be of relevance to the redox properties of the

**Scheme 1**

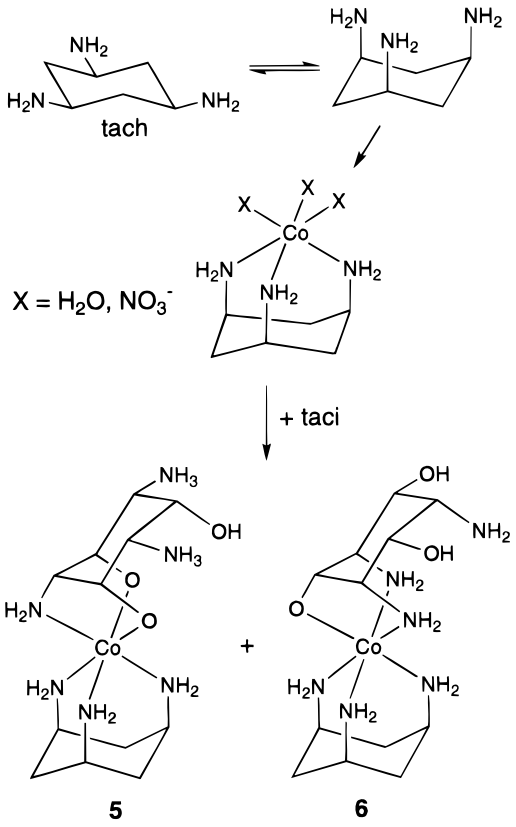


**Scheme 2**

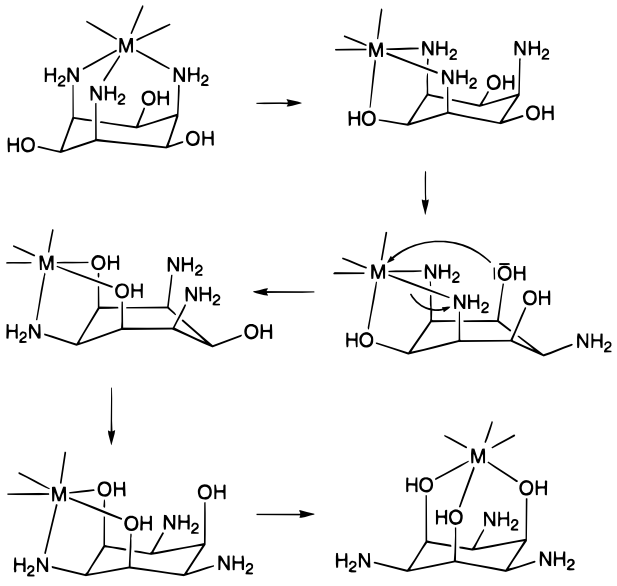

(33) Hegetschweiler, K.; Weber, M.; Huch, V.; Veith, M.; Schmalle, H. W.; Linden, A.; Geue, R. J.; Osvath, P.; Sargeson, A. M.; Willis, A. C.; Angst, W. *Inorg. Chem.* **1997**, *36*, 4121−4127.

(34) Hegetschweiler, K.; Ghisletta, M.; Hausherr-Primo, L.; Kradolfer, T.; Schmalle, H. W.; Gramlich, V. *Inorg. Chem.* **1995**, *34*, 1950.

Fe complex **2**. We recently showed for *cis*-inositol that an isomerization from a 1,3,5-triaxial to a 1,2,3-axial−equatorial−axial coordination mode is much faster than complete dissociation of the ligand.[12] This can be explained by the fact that only one metal−ligand bond must be broken during this isomerization reaction (rocking mechanism). It is likely that the structural rearrangement which may be required for the Fe−taci system occurs via a similar mechanism, rather than via complete dissociation and reassociation of the ligand, and the structures of **5** and **6** could serve as instructive models for corresponding intermediates (Scheme 2).

**Acknowledgment.** We thank Dr. Peter Osvath (CSIRO, Clayton, VIC, Australia) for his careful reading of the manuscript and Prof. Andreas Hauser (University of Geneva) for helpful discussion. Financial support from the Hungarian Research Foundation (OTKA, T022909, for L.N.), from Kredite für Unterricht und Forschung der ETH Zürich (for M.G.) and from Vifor (International) Inc. (for L.H.-P.) is gratefully acknowledged.

**Supporting Information Available:** Listings of crystallographic data, anisotropic displacement parameters, complete positional and thermal parameters, and bond distances and bond lengths (23 pages). Ordering information is given on any current masthead page.

IC971242B